

Triplet superconductivity in 3D Dirac semimetal due to exchange interaction.

Baruch Rosenstein,^{1,2,*} B. Ya. Shapiro,^{3,†} Dingping Li,^{4,5,‡} and I. Shapiro^{3,§}

¹*Electrophysics Department, National Chiao Tung University, Hsinchu 30050, Taiwan, R. O. C*

²*Physics Department, Ariel University, Ariel 40700, Israel*

³*Physics Department, Bar-Ilan University, 52900 Ramat-Gan, Israel*

⁴*School of Physics, Peking University, Beijing 100871, China*

⁵*Collaborative Innovation Center of Quantum Matter, Beijing, China*

Conventional phonon-electron interaction induces either triplet or one of two (degenerate) singlet pairing states in time reversal and inversion invariant 3D Dirac semi - metal. Investigation of the order parameters and energies of these states at zero temperature in wide range of values of chemical potential μ , the effective electron-electron coupling constant λ and Debye energy T_D demonstrates that when the exchange interaction is neglected the singlet always prevails, however in significant portions of the (μ, λ, T_D) parameter space the energy difference is very small. This means that interactions that are small but discriminate between the spin singlet and the spin triplet are important in order to determine the nature of the superconducting order there. The best candidate for such an interaction in materials under consideration is the exchange (the Stoner term) characterized by constant λ_{ex} . We show that at values of λ_{ex} much smaller than ones creating Stoner instability to ferromagnetism $\lambda_{ex} \sim 1$ the triplet pairing becomes energetically favored over the singlet ones for $\mu < T_D$. The 3D quantum critical point at $\mu = 0$ is considered in detail.

PACS numbers: 74.90.Rp 74.20.Fg, 74.90.+n, 74.40.Kb

I. INTRODUCTION.

Recently solids with electronic states described by the Bloch wave functions, obeying the "pseudo-relativistic" Dirac equation (with Fermi velocity v_F replacing the velocity of light) attracted widespread attention. One outstanding example is graphene, a two-dimensional (2D) hexagonal lattice made of carbon atoms. The effective low energy two-band model (near its K and K' points in the Brillouin zone) is described by the four-component (two pseudospins/sublattices and two valleys) massless 2D Dirac Hamiltonian (in fact there are two species of such quasiparticles for each spin). Although a similar two-band electronic structure of bismuth was described by a four-component nearly massless Dirac fermion in 3D caused by spin-orbit interaction long ago¹ (with spin replacing pseudospin), only recently several systems were experimentally found to exhibit the 3D Dirac quasiparticles. Their discovery followed recent exploration of the topological band theory².

One of the effective ideas to get a 3D Dirac semi-metal is to close the insulating gap by tuning a topological insulator towards the quantum phase transition to trivial insulators when the reflection symmetry is preserved³. The time reversal invariant 3D Dirac point in materials like Na_3Bi was theoretically investigated⁴ and experimentally observed⁵. A well known compound Cd_3As_2 is a symmetry-protected 3D Dirac semimetal with a single pair of Dirac points in the bulk and nontrivial Fermi arcs on the surface⁶. Most recently conductivity and magneto-absorption of a zinc-blende crystal, $HgCdTe$, was measured⁷ and is in agreement with theoretical expectations in Dirac semimetal⁸. Ab-initio calculations and symmetry arguments predict⁹ that cristobalite BiO_2 exhibits Dirac points at three symmetry related X points

on the boundary of the FCC Brillouin zone. Pyrochlore iridates¹⁰ and inverse perovskites¹¹ were also predicted to be Weyl - semimetals. Several known materials with well known magnetic or transport properties have recently undergone a "delayed" realization that they are actually Dirac semimetals¹².

The discovery of the 3D Dirac materials makes it possible to study their physics including remarkable electronic properties. This is rich in new phenomena, not seen in 2D Dirac semi - metals like graphene and surface states of topological insulator also harboring 2D Weyl quasiparticles. Examples include the giant diamagnetism that diverges logarithmically when the chemical potential approaches the 3D Dirac point; linear-in-frequency AC conductivity that has an imaginary part⁸; quantum magnetoresistance showing linear field dependence in the bulk¹¹. Most of the properties of these new materials were measured at relatively high temperatures. However some of the topological insulators and suspected 3D Dirac semi-metals exhibit superconductivity at about the liquid He temperature.

The well known topological insulator Bi_2Se_3 doped with Cu , becomes superconducting at $T_c = 3.8K$ ¹³. At present its pairing symmetry is unknown. Some experimental evidence¹⁴ point to a conventional phononic pairing mechanism. The spin independent part of the effective electron - electron interaction due to phonons was studied theoretically^{15,16}. For a conventional parabolic dispersion relation, typically independent of spin, the phonon mechanism leads to the s -wave superconductivity. The layered, non-centrosymmetric heavy element $PbTaSe_2$ was found to be superconducting¹⁷. Its electronic properties like specific heat, electrical resistivity, and magnetic-susceptibility indicate that $PbTaSe_2$ is a moderately coupled, type-II BCS superconductor with

large electron-phonon coupling constant of $\lambda = 0.74$. It was shown theoretically to possess a very asymmetric 3D Dirac point created by strong spin-orbit coupling. If the 3D is confirmed, it might indicate that the superconductivity is conventional phonon mediated.

More recently when the *Cu* doped *Bi₂Se₃* was subjected to pressure¹⁸, T_c increased to $7K$ at $30GPa$. Quasilinear temperature dependence of the upper critical field H_{c2} , exceeding the orbital and Pauli limits for the singlet pairing, points to the triplet superconductivity. The band structure of the superconducting compounds is apparently not very different from its parent compound *Bi₂Se₃*, so that one can keep the two band $\mathbf{k} \cdot \mathbf{p}$ description (*Se* p_z orbitals on the top and bottom layer of the unit cell mixed with its neighboring *Bi* p_z orbital). Electronic-structure calculations of the compound under pressure¹⁸ reveal a single bulk three-dimensional Dirac cone like in *Bi* with large spin-orbit coupling. Usually the phonon mediated pairing leads to the s -wave "conventional" superconductivity, while the p -wave pairing in *SrRuO₃* or heavy fermion superconductors like *UPt₃* "unconventional" nonphononic mechanism typically hinges on nonlocal interactions.

The case of the Dirac semi-metals is very special due to the strong spin dependence of the itinerant electrons' effective Hamiltonian. It was pointed out^{19,20} that in this case the triplet possibility can arise although the triplet gap is smaller than that of the singlet, the difference sometimes is not large for spin independent electron - electron interactions. Very recently the spin dependent part of the phonon induced electron - electron interaction was considered²¹ and it was shown that the singlet is still favored over the triplet pairing. Another essential spin dependent effective electron-electron interaction is the Stoner exchange among itinerant electrons²² leading to ferromagnetism in transition metals. While in the best 3D Weyl semimetal candidates it is too small to form a ferromagnetic state, it might be important to determine the nature of the superconducting condensate. Obviously it favors the triplet pairing.

It therefore of importance to clarify theoretically two questions. (i) Does a conventional phononic superconductivity exist in these materials with just a minute density of states compared even with high T_c cuprates that apparently utilize much more powerful pairing mechanism than phonons offer? (ii) Is it possible that phonons in 3D Dirac materials lead to triplet pairing that even becomes dominant under certain circumstances?

In the present paper we construct the theory of the superconducting transition in 3D Dirac semi-metal at arbitrary chemical potential including zero, assuming the local (probably, but not necessarily, phonon mediated) pairing. The possible pairing channels are classified in this rather unusual situation using symmetries of the system. In contrast to the 2D case, the triplet pairing is not only possible, but for a moderately strong exchange interaction is the preferred channel taking over the more "conventional" singlet one.

It turns out that the triplet superconductivity is easier realized in the intriguing case of a small chemical potential. The superconductivity there is governed by a quantum critical point (QCP)²³. The concept of QCP at zero temperature and varying doping constitutes a very useful language for describing the microscopic origin of superconductivity in high T_c cuprates and other "unconventional" superconductors²⁴. Quantum criticality, although occurring often in 2D (even in the context of surface superconductivity in topological insulators²⁵), is very rare in 3D. We find and characterize the quantum critical points corresponding to both the singlet and the triplet superconducting transitions. There are experimental methods to tune the chemical potential by doping (for example by copper¹³), gating²⁶, pressure¹⁸ etc.

The paper is organized as follows. The model of the phonon mediated and exchange effective local interactions of Dirac fermion is presented and the method of its solution (in the Gorkov equations form) including the symmetry analysis of possible pairing channels is given in Section II. In Section III the phase diagram for spin independent interactions is established and the regions in parameter space where singlet and triplet states are nearly degenerate are identified. The Stoner exchange interaction is considered perturbatively in Section IV. A novel case of zero chemical potential (QCP) is studied in Section V. Section VI contains discussion on experimental feasibility of the phonon mediated surface superconductivity in 3D Weyl semi-metals, as well as a comparison with earlier calculations and conclusion.

II. THE LOCAL PAIRING MODEL IN THE DIRAC SEMIMETAL.

A. Interactions in the Dirac semi-metal.

Electrons in the 3D Dirac semimetal are described by fields operators $\psi_{fs}(\mathbf{r})$, where $f = L, R$ are the valley index (pseudospin) for the left/right chirality bands with spin projections taking the values $s = \uparrow, \downarrow$ with respect to, for example, z axis. To use the Dirac ("pseudo-relativistic") notations, these are combined into a four component bi-spinor creation operator, $\psi^\dagger = (\psi_{L\uparrow}^\dagger, \psi_{L\downarrow}^\dagger, \psi_{R\uparrow}^\dagger, \psi_{R\downarrow}^\dagger)$, whose index $\gamma = \{f, s\}$ takes four values. The non-interacting massless Hamiltonian with Fermi velocity v_F and chemical potential μ reads⁴,

$$K = \int_{\mathbf{r}} \psi^\dagger(\mathbf{r}) \widehat{K} \psi(\mathbf{r}); \quad \widehat{K}_{\gamma\delta} = -i\hbar v_F \nabla^i \alpha_{\gamma\delta}^i - \mu \delta_{\gamma\delta}, \quad (1)$$

where three 4×4 matrices, $i = x, y, z$,

$$\alpha = \begin{pmatrix} \sigma & 0 \\ 0 & -\sigma \end{pmatrix}, \quad (2)$$

are presented in the block form via Pauli matrices σ . They are related to the Dirac γ matrices (in the chiral

representation, sometimes termed "spinor") by $\alpha = \beta\gamma$ with

$$\beta = \begin{pmatrix} 0 & \mathbf{1} \\ \mathbf{1} & 0 \end{pmatrix}. \quad (3)$$

Here $\mathbf{1}$ is 2×2 identity matrix.

We consider a special case of 3D rotational symmetry that in particular has an isotropic Fermi velocity. Moreover we assume the time reversal, $\Theta\psi(\mathbf{r}) = i\sigma_y\psi^*(\mathbf{r})$, and inversion symmetries although the pseudo Lorentz symmetry will be explicitly broken by interactions. The spectrum of single particle excitations is linear, see Fig.1. The chemical potential μ is counted from the Dirac point.

Electrons interact electrostatically via the density - density potential $v(\mathbf{r})$:

$$V_{e-e} = \frac{1}{2} \int_{\mathbf{r}\mathbf{r}'} \rho(\mathbf{r}) v(\mathbf{r} - \mathbf{r}') \rho(\mathbf{r}'); \quad (4)$$

$$\rho(\mathbf{r}) = \psi_{\alpha}^{\dagger}(\mathbf{r}) \psi_{\alpha}(\mathbf{r}) = \psi_{Ls}^{\dagger} \psi_{Ls} + \psi_{Rs}^{\dagger} \psi_{Rs}$$

In Weyl semi-metals there is no static screening at $\mu = 0$, although dynamically it is screened within RPA¹⁰. The screening length is therefore not small like in good metals. However in most materials that realize the Dirac semi - metals¹¹, there is a large dielectric constant $\epsilon \sim 50$ that allows phonon - electron coupling²⁷,

$$H_{e-ph} = w \int \rho(\mathbf{r}) \nabla \cdot \mathbf{u}(\mathbf{r}), \quad (5)$$

to overpower it to create the Cooper pairs as mentioned in Introduction. Here $\mathbf{u}(\mathbf{r})$ denotes the displacement of ions and the electron-ion coupling $w \propto M^{-1/2}$, where M is the ion mass. The effective electron-electron interaction due to both electron - phonon attraction and Coulomb repulsion (pseudopotential) can be generally expanded in derivatives. The leading term usually called the local (or the s -wave pairing) coupling is

$$V_{eff} = -\frac{g}{2} \int_{\mathbf{r}\mathbf{r}'} \rho(\mathbf{r}) \delta(\mathbf{r} - \mathbf{r}') \rho(\mathbf{r}') = \quad (6)$$

$$= -\frac{g}{2} \int_{\mathbf{r}} \psi_{\alpha}^{\dagger}(\mathbf{r}) \psi_{\beta}^{\dagger}(\mathbf{r}) \psi_{\beta}(\mathbf{r}) \psi_{\alpha}(\mathbf{r}). \quad (7)$$

Unlike the free Hamiltonian K , Eq.(1), this interaction Hamiltonian does not mix different spin components.

Such a coupling implicitly restricts the spin independent local interaction to be symmetric under the band permutation (the constants in front of the interband $\psi_1^{\dagger}\psi_1\psi_2^{\dagger}\psi_2$ and intraband $\psi_1^{\dagger}\psi_1\psi_1^{\dagger}\psi_1$ terms are the same). If the mechanism of pairing is due to acoustic phonons only, such an additional term is not generated. A more general case with additional independent term was considered in ref.¹⁹.

Usually such coupling with a positive coupling constant g leads to the s -wave "conventional" pairing, while an "unconventional" p -wave pairing in $SrRuO_3$ or heavy fermion superconductors like UPt_3 requires subleading

interaction terms with two derivatives (most probably beyond electron - phonon mechanism). Two qualitatively different cases will be considered, see Fig.1. When the chemical potential μ is much larger than the Debye energy T_D characterizing the outreach of the phonon - electron coupling, see Fig.1a, the physics is similar to that considered for the parabolic bands within the BCS approximations²⁷. The opposite case, $\mu < T_D$ (Fig. 1b) is unusual and most of our findings are devoted to this case.

The Coulomb forces in Eq.(4) in addition to direct repulsion lead to spin dependent forces due to exchange. The exchange interaction among itinerant electrons first considered by Stoner²², although small and unable to form a ferromagnetic state in materials under consideration, will be important for the nature of the condensate since it will lift the degeneracy between the singlet and the triplet pairing:

$$V_{s-s} = -\frac{1}{2} \int_{\mathbf{r},\mathbf{r}'} J(\mathbf{r} - \mathbf{r}') \mathbf{S}(\mathbf{r}) \cdot \mathbf{S}(\mathbf{r}'). \quad (8)$$

Spin density in Dirac semi-metal has the form

$$\mathbf{S}(\mathbf{r}) = \psi^{\dagger}(\mathbf{r}) \boldsymbol{\Sigma} \psi(\mathbf{r}), \quad (9)$$

where the matrices

$$\boldsymbol{\Sigma} = -\alpha\gamma_5 = \begin{pmatrix} \sigma & 0 \\ 0 & \sigma \end{pmatrix}; \quad \gamma_5 = \begin{pmatrix} -1 & 0 \\ 0 & 1 \end{pmatrix}, \quad (10)$$

are also the rotation generators.

B. The symmetry classification of possible pairing channels.

Since we consider the local interactions as dominant, the superconducting condensate (the off-diagonal order parameter) will be local

$$O = \int_{\mathbf{r}} \psi_{\alpha}^{\dagger}(\mathbf{r}) M_{\alpha\beta} \psi_{\beta}^{\dagger}(\mathbf{r}), \quad (11)$$

where the constant matrix M should be a 4×4 anti-symmetric matrix. Due to the rotation symmetry they transform covariantly under infinitesimal rotations generated by the spin S^i operator, Eq.(9) :

$$\int_{\mathbf{r},\mathbf{r}'} \left[\psi_{\alpha}^{\dagger}(\mathbf{r}) M_{\alpha\beta} \psi_{\beta}^{\dagger}(\mathbf{r}), \psi_{\gamma}^{\dagger}(\mathbf{r}') \boldsymbol{\Sigma}_{\gamma\delta}^i \psi_{\delta}(\mathbf{r}') \right] \quad (12)$$

$$= \int_{\mathbf{r}} \psi_{\gamma}^{\dagger}(\mathbf{r}) \boldsymbol{\Sigma}_{\gamma\delta}^i \{ M_{\delta\kappa}^t - M_{\delta\kappa} \} \psi_{\kappa}^{\dagger}(\mathbf{r}). \quad (13)$$

The representations of the rotation group therefore characterize various possible superconducting phases.

Out of 16 matrices of the four dimensional Clifford algebra six are antisymmetric and one finds one vector and three scalar multiplets of the rotation group. The multiplets contain:

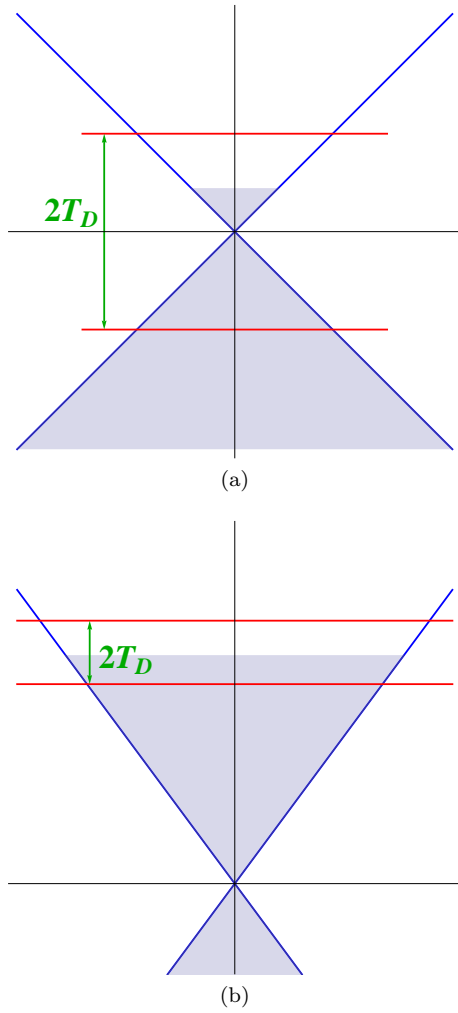


FIG. 1. Chemical potential in Dirac semi - metals and the phonon mediated pairing. (a) Chemical potential relative to Dirac point is smaller than typical energy of phonons, the Debye energy T_D . (b) The BCS approximation limit: the chemical potential is much larger than the Debye energy T_D .

(i) a triplet of order parameters:

$$\{M_x^T, M_y^T, M_z^T\} = \{\beta\alpha_z, -i\beta\gamma_5, \beta\alpha_x\} \quad (14)$$

The algebra is

$$[M_i^T, \Delta_j^T] = i\varepsilon_{ijk}M_k^T. \quad (15)$$

(ii) three singlets

$$M_1^S = i\alpha_y; \quad M_2^S = i\Sigma_y; \quad M_3^S = -i\beta\alpha_y\gamma_5. \quad (16)$$

Which one of the condensates is realized at zero temperature is determined by the parameters of the Hamiltonian and is addressed within the Gaussian approximation next.

III. THE PHASE DIAGRAM FOR SPIN INDEPENDENT INTERACTIONS.

A. Gorkov equations.

The BCS type approximation can be employed. Using the standard formalism, the Matsubara Green's functions (τ is the Matsubara time)

$$G_{\alpha\beta}(\mathbf{r}, \tau; \mathbf{r}', \tau') = -\langle T_\tau \psi_\alpha(\mathbf{r}, \tau) \psi_\beta^\dagger(\mathbf{r}', \tau') \rangle; \quad (17)$$

$$F_{\alpha\beta}^\dagger(\mathbf{r}, \tau; \mathbf{r}', \tau') = \langle T_\tau \psi_\alpha^\dagger(\mathbf{r}, \tau) \psi_\beta^\dagger(\mathbf{r}', \tau') \rangle,$$

obey the Gor'kov equations²⁷:

$$\begin{aligned} & -\frac{\partial G_{\gamma\kappa}(\mathbf{r}, \tau; \mathbf{r}', \tau')}{\partial \tau} - \int_{\mathbf{r}''} \langle \mathbf{r} | \widehat{K}_{\gamma\beta} | \mathbf{r}'' \rangle G_{\beta\kappa}(\mathbf{r}'', \tau; \mathbf{r}', \tau') \\ & - gF_{\beta\gamma}(\mathbf{r}, \tau; \mathbf{r}, \tau) F_{\beta\kappa}^\dagger(\mathbf{r}, \tau; \mathbf{r}', \tau') = \delta^{\gamma\kappa} \delta(\mathbf{r} - \mathbf{r}') \delta(\tau - \tau'); \\ & \frac{\partial F_{\gamma\kappa}^\dagger(\mathbf{r}, \tau; \mathbf{r}', \tau')}{\partial \tau} - \int_{\mathbf{r}''} \langle \mathbf{r} | \widehat{K}_{\gamma\beta}^t | \mathbf{r}'' \rangle F_{\beta\kappa}^\dagger(\mathbf{r}'', \tau; \mathbf{r}', \tau') \\ & - gF_{\gamma\beta}^\dagger(\mathbf{r}, \tau; \mathbf{r}, \tau) G_{\beta\kappa}(\mathbf{r}, \tau; \mathbf{r}', \tau') = 0. \end{aligned} \quad (18)$$

In the homogeneous case the Gor'kov equations for Fourier components of the Greens functions simplify considerably,

$$D_{\gamma\beta}^{-1} G_{\beta\kappa}(\omega, p) - \Delta_{\gamma\beta} F_{\beta\kappa}^\dagger(\omega, p) = \delta^{\gamma\kappa}; \quad (19)$$

$$D_{\beta\gamma}^{-1} F_{\beta\kappa}^\dagger(\omega, p) + \Delta_{\gamma\beta}^* G_{\beta\kappa}(\omega, p) = 0,$$

where $\omega = \pi T(2n+1)$ is the Matsubara frequency and $D_{\gamma\beta}^{-1} = (i\omega - \mu) \delta_{\gamma\beta} + v_F p^j \alpha_{\gamma\beta}^j$.

The matrix gap function can be chosen as (d is real)

$$\Delta_{\beta\gamma} = gF_{\gamma\beta}(0) = gdM_{\gamma\beta}. \quad (20)$$

These equations are conveniently presented in matrix form (superscript t denotes transposed and I - the identity matrix):

$$\begin{aligned} D^{-1}G - \Delta F^\dagger &= I; \\ D^{t-1}F^\dagger + \Delta^*G &= 0. \end{aligned} \quad (21)$$

Solving these equations one obtains

$$\begin{aligned} G^{-1} &= D^{-1} + \Delta D^t \Delta^*; \\ F^\dagger &= -D^t \Delta^* G, \end{aligned} \quad (22)$$

with the gap function found from the consistency condition

$$\Delta^* = -g \sum_{\omega q} D^t \Delta^* G. \quad (23)$$

Now we find solutions of this equation for each of the possible superconducting phases.

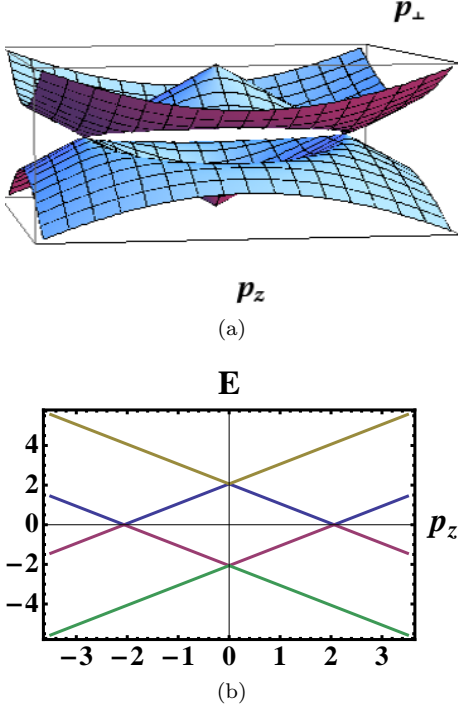


FIG. 2. Spectrum of triplet excitations (a) section $p_{\perp} = 0$. (b) There is also a saddle points with energy gap.

B. Triplet solution of gap equation.

In this phase rotational symmetry is spontaneously broken simultaneously with the electric charge $U(1)$ (global gauge invariance) symmetry. Assuming z direction of the p -wave condensate the order parameter matrix takes a form: $\Delta = \Delta_T M_z^T = \Delta_T \beta \alpha_x$. In this Section we use the units of $v_F = 1, \hbar = 1$ and the energy scale will be set by the Debye cutoff, $T_D = 1$, of the electron-phonon interactions, see below. The off-diagonal (41) matrix element of the matrix gap equation, Eq.(23), for real $\Delta_T > 0$ is:

$$\frac{1}{g} = \sum_{\omega q} (\Delta_T^2 + p_{\perp}^2 - p_z^2 + \mu^2 + \omega^2) \times \left[(\Delta_T^2 + \omega^2)^2 + (p^2 - \mu^2)^2 + 2(p^2 + \mu^2)\omega^2 + 2\Delta_T^2(p_{\perp}^2 - p_z^2 + \mu^2) \right]^{-1}, \quad (24)$$

where $p_{\perp}^2 = p_x^2 + p_y^2$. The spectrum of elementary excitations obtained from the four poles of the Green's function, see Fig.2, is (in physical units)

$$E_{\pm}^2 = \Delta_T^2 + v_F^2 p^2 + \mu^2 \pm 2v_F \sqrt{\Delta_T^2 p_z^2 + p^2 \mu^2}. \quad (25)$$

There are two nodes at $p_x = p_y = 0, v_F p_z = \pm \sqrt{\Delta_T^2 + \mu^2}$, when the branches $+|E_-|$ and $-|E_-|$ cross, see Fig.2a and a section $p_{\perp} = 0$ in Fig.2b. There is also a saddle point with energy gap, $2\Delta_T$ on the circle

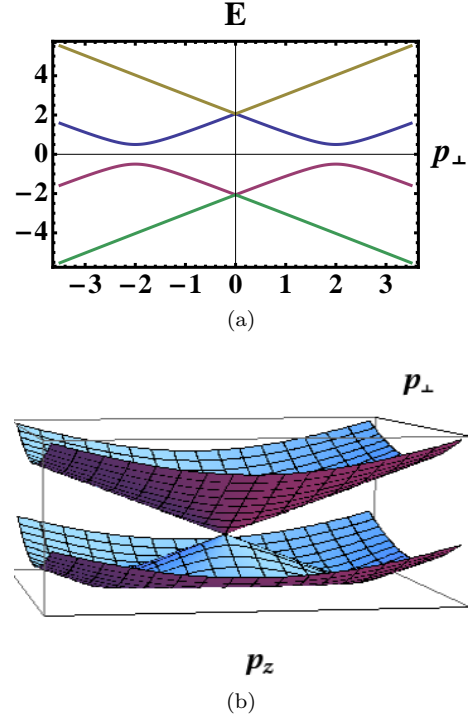


FIG. 3. Spectrum of triplet excitations (a) $2\Delta_T$ on the circle $p_x^2 + p_y^2 = \mu^2, p_z = 0$ see the section in the $p_z = 0$ direction. (b) The higher energy band E_+ touches the lower band at $p = 0$, so that there is a Dirac point for quasiparticles.

$p_x^2 + p_y^2 = \mu^2, p_z = 0$, see the section in the $p_z = 0$ direction in Fig. 3a. The higher energy band E_+ touches the lower band at $p = 0$, so that there is a Dirac point for quasiparticles, see Fig. 3b.

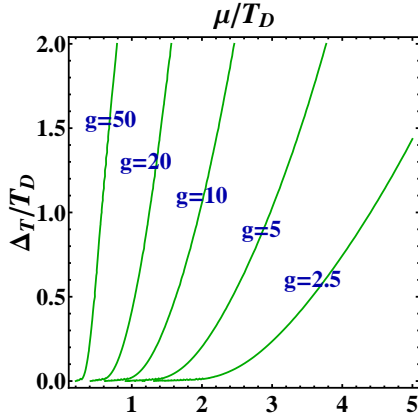
Integration over ω , using polar coordinates for p and $x = \cos \theta, \zeta = \sqrt{\Delta_T^2 x^2 + \mu^2}$, gives

$$\frac{1}{g} = \frac{1}{8\pi^2} \int_{p=\max[\mu-1,0]}^{\mu+1} \int_{x=0}^1 \frac{p^2}{\zeta} \left\{ \frac{\zeta + px^2}{\sqrt{\Delta_T^2 + p^2 + \mu^2 + 2p\zeta}} + \frac{\zeta - px^2}{\sqrt{\Delta_T^2 + p^2 + \mu^2 - 2p\zeta}} \right\}. \quad (26)$$

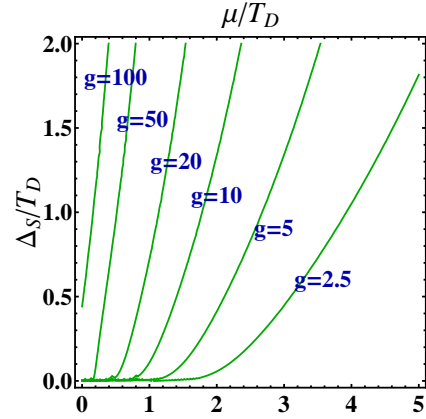
The lower bound on the momentum integration is nonzero when the chemical potential μ exceeds T_D . The integral over x was performed analytically, while the last integral was done numerically. The result of the numerical solution of the gap equation for Δ_T is presented in Fig.4a. The lines of fixed g in the $\mu - \Delta_T$ plane are shown. As expected the gap increases as a function of μ . However, when the same is replotted as lines of fixed phonon-electron coupling,

$$\lambda = gD(\mu) = g\mu^2 / (8\pi^2 v_F^3 \hbar^3), \quad (27)$$

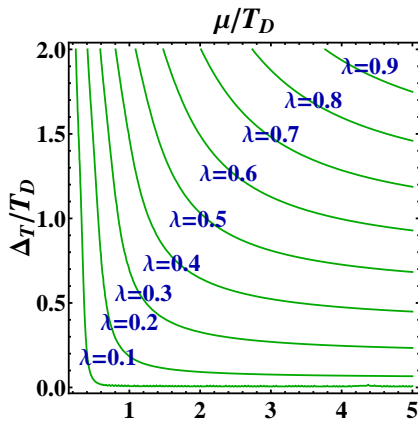
the gap increases upon reduction in μ , see Fig.4b. At large $\mu \gg T_D$ the gap becomes independent of μ as in BCS, discussed next.



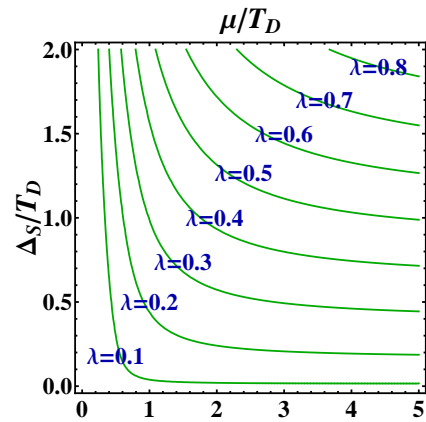
(a)



(a)



(b)



(b)

FIG. 4. Triplet order parameter Δ_T . (a) as function of λ , (b) as function of g .

FIG. 5. Singlet order parameter Δ_S . (a) as function of λ , (b) as function of g .

In several limiting cases the integrals can be performed analytically. At zero chemical potential the results are presented in Section IV, while here we list the BCS limit of $\mu \gg T_D$ and the strong coupling case of $g\mu^2 \gg 1, \Delta_T \propto g$.

(i) In the BCS limit one has

$$\frac{1}{g} = \frac{a_T \mu^2}{4\pi^2} \sinh^{-1} \frac{T_D}{\Delta_T}, \quad (28)$$

with $a_T = 0.69$, leading to an exponential gap dependence on λ when it is small:

$$\Delta_T = T_D / \sinh(1/2a_T\lambda) \simeq 2T_D e^{-1/2a_T\lambda}. \quad (29)$$

(ii) In the strong coupling one obtains with solution

$$\Delta_T = \frac{g}{12\pi^2} \begin{cases} 6\mu^2 + 2 & \text{for } \mu < 1 \\ (\mu + 1)^3 & \text{for } \mu > 1 \end{cases}, \quad (30)$$

see Fig.4a. Usually the local coupling does not prefer the triplet pairing and the singlet channels of coupling are realized. We therefore turn to them.

C. Singlet representations.

It turns out that the second singlet in Eq.(16) gives results identical to that of the first one, while the third singlet does not have a solution in the physically interesting range of parameters. Therefore we assume the order parameter in the matrix form $\Delta = \Delta_S M_1^S = i\Delta_S \alpha^y$. The relevant (41) matrix element of the matrix gap equation, Eq.(23), is for real Δ_S :

$$\frac{1}{g} = \sum_{\omega p} (\Delta_S^2 + p^2 + \mu^2 + \omega^2) \times \left[(\Delta_S^2 + p^2)^2 + (\mu^2 + \omega^2 + 2\Delta_S^2)(\mu^2 + \omega^2) + 2p^2(\omega^2 - \mu^2) \right]^{-1}. \quad (31)$$

The spectrum (in physical units) now is isotropic,

$$E_{\pm}^2 = \Delta_S^2 + (v_F |p| \pm \mu)^2. \quad (32)$$

Integration over ω gives

$$\frac{1}{g} = \mu \sum_{\mu - T_D < \varepsilon_p < \mu + T_D} \frac{p}{r_+ r_- (r_+ - r_-)}, \quad (33)$$

where $r_{\pm} = \sqrt{\Delta_S^2 + (|p| \pm \mu)^2}$, while the p integration results in:

$$\begin{aligned} \frac{16\pi^2}{g} &= \Phi(\mu + 1) - \Phi(\max[\mu - 1, 0]); \\ \Phi(\mu) &= r_- (p + 3\mu) + r_+ (p - 3\mu) - (\Delta_S^2 - 2\mu^2) \\ &\quad \times \log[(p + r_- - \mu)(p + r_+ + \mu)]. \end{aligned} \quad (34)$$

The solution is presented in Fig. 5a and 5b as lines of constant g and λ , respectively. One observes that the gaps are comparable to those of the triplet shown in Fig.4 in whole range of parameters. The expression for the gap simplifies for

(i) BCS, $\mu \gg T_D$

$$\Delta_S = T_D / \sinh(1/2\lambda) \simeq 2T_D e^{-1/2\lambda}. \quad (35)$$

(ii) Strong coupling

$$\Delta_S = \frac{2\lambda(T_D + \mu)^3}{3\mu^2}. \quad (36)$$

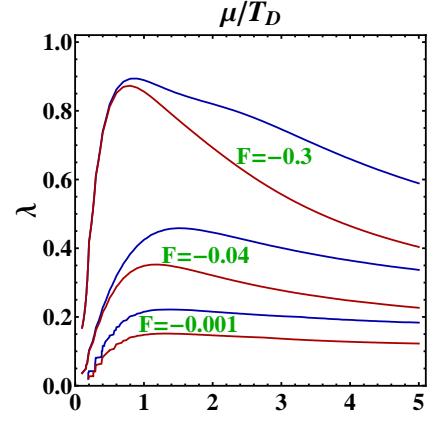
Having found the order parameter, one has to determine what symmetry breaking is realized by comparing energies of the solutions.

IV. SINGLET VS TRIPLET. ENERGY.

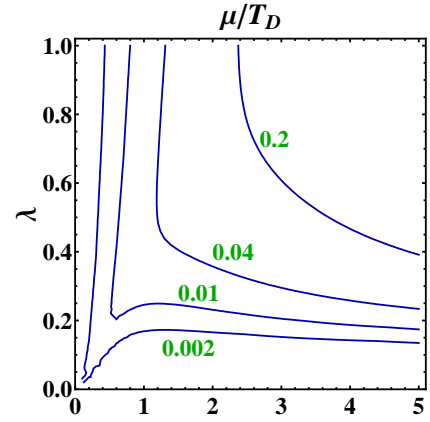
We calculate the energy of a solution using the well known formula²⁷

$$F = 2 \int_{\Delta'=0}^{\Delta} \frac{d(1/g)}{d\Delta'} \Delta'^2. \quad (37)$$

For the triplet and singlet solutions the result of integration performed numerically is presented in Fig.6a. One observes that for all but the smallest coupling λ the channels are nearly degenerate although the singlet is always lower. The lines of constant difference $F_T - F_S$ are given in Fig. 6b as functions of μ and λ . As can be seen, the difference becomes small especially at smaller chemical potential. In Fig.7 more detailed results for the triplet and the singlet order parameters are presented for chemical potential smaller than Debye energy. One clearly observes the critical values of $8\pi^2$ and $12\pi^2$ for couplings g when the singlet and triplet appears. They become nearly degenerate just above $12\pi^2$. Energies are also nearly degenerate. The case of the quantum critical point $\mu = 0$ is considered in detail analytically in the following Section.



(a)



(b)

FIG. 6. Energy of triplet and singlet. (a) Profile of constant energy for singlet and triplet condensates in the $\mu - \lambda$ plane. (b) Difference $F_T - F_S$.

In limiting cases, one obtains expressions in closed form.

(i) BCS, $\mu > T_D$, using Eq.(28) and Eq.(29) for the triplet and Eq.(35) for the singlet, one has the energy density:

$$\begin{aligned} F_{T,S} &= -\frac{a_{T,S} \mu^2 T_D}{2\pi^2 v_F^3 \hbar^3} \left(\sqrt{\Delta_T^2 + T_D^2} - T_D \right) \\ &\simeq -\frac{a_{T,S}}{\pi^2} \frac{\mu^2 T_D^2}{v_F^3 \hbar^3} \exp\left(-\frac{1}{a_{T,S} \lambda}\right), \end{aligned} \quad (38)$$

with $a_T = 0.69$, while $a_S = 1$ and assuming $\lambda \ll 1$. The ratio of the two phases gives

$$\frac{F_T}{F_S} = 0.69 e^{-0.45/\lambda}. \quad (39)$$

(ii) Strong coupling limit, using Eq.(30) for triplet and Eq.(36) for the singlet,

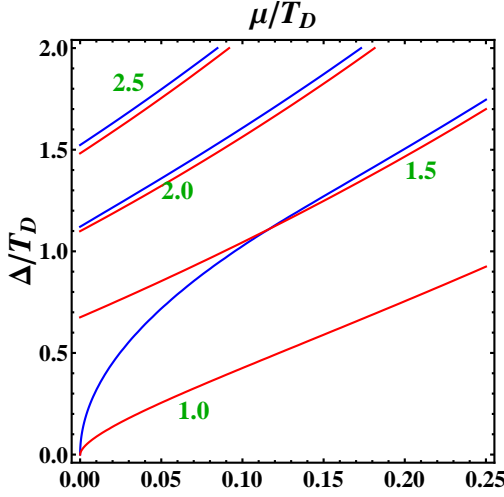


FIG. 7. Order parameters for triplet and singlet near criticality. Order parameters of triplet (blue) and singlet at following values of coupling constant (in units of critical value for singlet g_c^S): 1, 3/2 (critical value for triplet), 2, 5/2.

$$F_T = F_S = -\frac{1}{72\pi^4 v_F^3 \hbar^3} \begin{cases} 4(3\mu^2 + T_D^2)^2 & \text{for } \mu < T_D \\ T_D^{-2}(\mu + T_D)^6 & \text{for } \mu > T_D \end{cases}. \quad (40)$$

The difference appears at order $1/g$.

To summarize, in most of the parameter range shown triplet is a bit higher than that of the singlet, but the two condensates are nearly degenerate. The degeneracy in practise is lifted in favor of the triplet by the spin-spin interaction, Eq.(8), or magnetic impurities present in materials exhibiting the 3D Dirac point.

A. The influence of exchange.

Let us estimate the perturbatively the energy change due to the exchange interactions due to Stoner exchange. In the simplest case of local spin attraction one uses the Stoner approximation²², $J(\mathbf{r}) = I\delta(\mathbf{r})$, where I is the Stoner constant, using the Gaussian factorization one obtains

$$\begin{aligned} \delta F &= -\frac{I}{2V} \int_{\mathbf{r}} \Sigma_{\alpha\beta}^i \Sigma_{\gamma\delta}^i \langle \psi_{\alpha}^+(r) \psi_{\beta}(r) \psi_{\gamma}^+(r) \psi_{\delta}(r) \rangle \\ &\simeq \frac{I}{2V} \int_{\mathbf{r}} \Sigma_{\alpha\beta}^i \Sigma_{\gamma\delta}^i \langle \psi_{\alpha}^+(r) \psi_{\gamma}^+(r) \rangle \langle \psi_{\beta}(r) \psi_{\delta}(r) \rangle \\ &= \frac{I}{2g^2} \Delta_{\gamma\alpha}^* \Sigma_{\alpha\beta}^i \Delta_{\beta\delta} \Sigma_{\delta\gamma}^{it}. \end{aligned} \quad (41)$$

The triplet, $\Delta = \Delta_T \beta \alpha^x$, predictably gains energy

$$\delta F_T = -\frac{2I}{g^2} \Delta_T^2, \quad (42)$$

while singlet, $\Delta = i\Delta_S \alpha^y$ loses energy

$$\delta F_S = \frac{6I}{g^2} \Delta_S^2. \quad (43)$$

As in the case of the phonon induced interactions, a more convenient dimensionless quantity describing the exchange is

$$\lambda_{ex} = ID(\mu) = I\mu^2 / (8\pi^2 v_F^3 \hbar^3). \quad (44)$$

We assume that the value is quite far from the Stoner ferromagnetic instability value ($\lambda_{ex} = 1$). The gain of triplet over the singlet is therefore written as

$$\delta F_T - \delta F_S = -\frac{2\lambda_{ex}}{\lambda^2} D(\mu) (\Delta_T^2 + 3\Delta_S^2),$$

and is given in Fig.8a. The difference of full energies is given in Figs.8b-8c for two values of the exchange coupling. The crossover from singlet to triplet occurs, $F_T + \delta F_T = F_S + \delta F_S$ at the following value of the exchange coupling:

$$\lambda_{ex}^c = \frac{\lambda^2}{2D(\mu)} \frac{F_T - F_S}{3\Delta_S^2 + \Delta_T^2}. \quad (45)$$

In the general case two values of exchange coupling were calculated numerically leading to the phase diagram shown in Fig. 9. General feature of the phase diagram is that the triplet superconductivity might appear either at small chemical potential or at very large one compared to T_D . The second possibility is not realized. Since perturbation theory in exchange coupling was used, the estimate is valid only when $F_{S,T} \gg \delta F_{S,T}$ marked by dashed lines on Fig.8b,c. On the lines the perturbation is half of the leading order. We argue that in this region either a ferromagnetic state is formed or the perturbation theory is not valid. In limiting cases analytic expression can be obtained.

(i) For $\mu \gg T_D$ according to Eq.(38)

$$F_T + \delta F_T = -8D(\mu) T_D^2 \left(a_T + \frac{\lambda_{ex}}{\lambda^2} \right) e^{-1/a_T \lambda}; \quad (46)$$

$$F_S + \delta F_S = -8D(\mu) T_D^2 \left(1 - 3\frac{\lambda_{ex}}{\lambda^2} \right) e^{-1/\lambda}.$$

Therefore the transition occurs when

$$\lambda_{ex}^c = \lambda^2 \frac{e^{(a_T^{-1}-1)/\lambda} - a_T}{3e^{(a_T^{-1}-1)/\lambda} + 1} \approx \frac{\lambda^2}{3}. \quad (47)$$

(ii) In the strong coupling for $\mu \ll T_D$, $\Delta_T = \Delta_S \sim \frac{T_D^4}{18\pi^4 v_F^3 \hbar^3}$, so that the difference is

$$\delta F_T - \delta F_S \sim -\frac{32}{9\pi^2} \frac{\lambda_{ex} T_D^4}{\mu^2}. \quad (48)$$

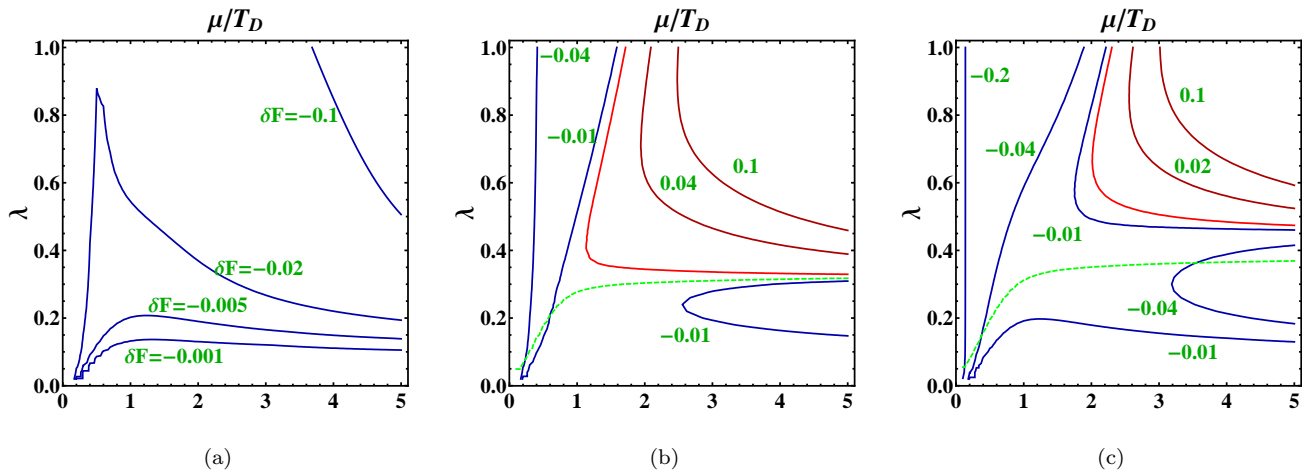


FIG. 8. Comparison between energies of the singlet and triplet. (a) Exchange corrections difference between the two channels: $\delta F = \delta F_T - \delta F_S$. (b) Difference of energies including the exchange correction for $\lambda_{ex} = 0.02$. The red line separates the singlet phase from the triplet phase. Above the line on the brown curves the energy difference $F_T - F_S$ is positive, while below it on the green line it is negative. Portion of the phase diagram below the dashed line requires consideration beyond perturbation theory. (c) Same for much larger exchange coupling $\lambda_{ex} = 0.32$.

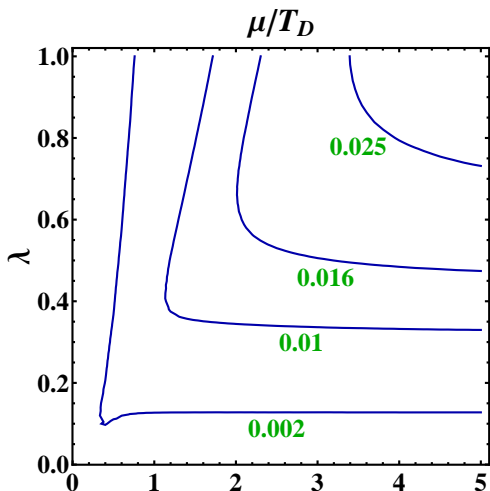


FIG. 9. Critical exchange coupling for various chemical potential μ and the phonon induced electron-electron coupling λ .

The triplet is always favored in this limit due to degeneracy of energies without the exchange coupling.

As is seen from figure 8 the most promising region in parameter space in which the triplet superconductivity prevails is at small chemical potential. As was mentioned in Introduction, the "extreme" case of zero chemical potential can be physically achieved by tuning parameters of the material to the transition between the topological insulator phase and the band insulator phase, so we study it in more detail.

V. QUANTUM CRITICAL POINT AT ZERO CHEMICAL POTENTIAL AND ITS CRITICAL EXPONENTS.

A peculiarity of superconductivity in Dirac semimetal at zero chemical potential is that electrons (and holes) in Cooper pairs are created themselves by the pairing interaction rather than being present in the sample as free electrons. Therefore it is shown that it is possible to neglect the effect of weak doping and consider directly the $\mu = 0$ particle-hole symmetric case. This point in parameter space is the QCP²³. Microscopically, Cooper pairs of both electrons and holes are formed. The system is unique in this sense since the electron - hole symmetry is not spontaneously broken in both normal and superconducting phases. Supercurrent in such a system does not carry momentum or mass. We discuss the triplet state followed by the singlet.

A. Triplet.

Spectrum of the triplet becomes very simple, $E_{\pm}^2 = (\Delta_T \pm v_F |p_z|)^2 + v_F^2 p_{\perp}^2$. Performing analytically the integral over the angle and momentum in the gap equation, Eq.(26), one obtains

$$\frac{12\pi^2 v_F^3 \hbar^3}{g} = \begin{cases} T_D^2 - \frac{\Delta_T^2}{5} & \text{for } \Delta_T < T_D \\ \frac{T_D^3}{\Delta_T} - \frac{T_D^5}{5\Delta_T^3} & \text{for } \Delta_T > T_D \end{cases}. \quad (49)$$

The solution of the equation for Δ_T as function of coupling g is presented in Fig. 10a. The triplet superconducting solution exists, like in the 2D case²⁵, only when

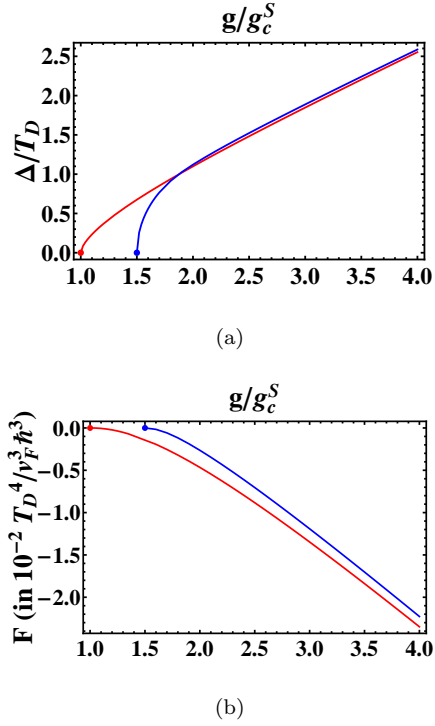


FIG. 10. Quantum critical point $\mu = 0$. (a) Singlet and triplet order parameter as function of g . (b) Energies.

the coupling exceeds a critical value (in physical units),

$$g_c^T = 12\pi^2 \frac{v_F^3 \hbar^3}{T_D^2}. \quad (50)$$

The dependence on the cutoff T_D is incorporated in the renormalized coupling with dimension of energy defined as

$$U_T^2 = T_D^2 \left(1 - \frac{g_c^T}{g}\right). \quad (51)$$

This quantity can be interpreted as an effective binding energy of the Cooper pair in the Dirac semi-metal. The dependence of the gap is $\Delta_T = \sqrt{5}U_T$ for $U_T < 5^{-1/2}$ (or $g < 5/4g_c^T$). The critical exponent therefore is $\Delta_T \propto (1 - g_c^T/g)^\beta$ for $\beta = 1/2$. This defines the (zero temperature) triplet quantum critical point.

Energy, calculated using the AGD formula, Eq.(37), can be written via the energy gap in a closed form:

$$F_T = -\frac{T_D^2}{5g_c^T} \begin{cases} \frac{\Delta_T^4}{T_D^4} & \text{for } \Delta_T < T_D \\ 10\frac{\Delta_T}{T_D} - 15 + \frac{6T_D}{\Delta_T} & \text{for } \Delta_T > T_D \end{cases}. \quad (52)$$

Near criticality, Eq.(52), $F_T \propto (1 - g_c^T/g)^{2-\alpha}$, determines the quantum critical exponent $\alpha = 2$. Critical exponents coincide with the classical mean field 3D exponents.

In the strong coupling limit $\Delta_T = T_D g/g_c^T$ and $F_T = -2gT_D^2/(g_c^T)^2$. As we see in the next subsection, the

triplet QCP is unstable since the singlet order parameter solution has lower energy.

B. Singlet.

The spectrum is relativistic with the rest mass equal to the gap, $E^2 = \Delta_S^2 + v_F^2 p^2$. The gap equation after integrations is

$$\frac{8\pi^2 v_F^3 \hbar^3}{g} = T_D \sqrt{\Delta_S^2 + T_D^2} - \Delta_S^2 \sinh^{-1}(T_D/\Delta_S). \quad (53)$$

The critical value is therefore lower than that for the triplet

$$g_c^S = 8\pi^2 \frac{v_F^3 \hbar^3}{T_D^2}. \quad (54)$$

In terms of the renormalized coupling, $U_S^2 = T_D^2 \left(1 - \frac{g_c^S}{g}\right)$, the gap equation near criticality takes the form

$$U_S^2 = \Delta_S^2 \log\left(\frac{2T_D}{\sqrt{e}\Delta_S}\right). \quad (55)$$

The solution of Eq.(53) is given in Fig. 10a (red curve).

At small deviations from criticality one can approximate solution as $\Delta_S = U_S \log^{-1/2}(2T_D/\sqrt{e}U_S)$, while in the strong coupling limit, $\Delta_S = \frac{2g}{3g_c^S} T_D$. The energy is

$$F_S = \frac{2T_D}{g_c^S} \left(T_D - \sqrt{\Delta_S^2 + T_D^2}\right) + \frac{1}{g} \Delta_S^2. \quad (56)$$

Near critical coupling, $F_S \simeq -\frac{U_S^4}{T_D^2 g_c^S} \log^{-1}(2T_D/\sqrt{e}U_S)$, while in the strong coupling limit one obtains again degeneracy with the triplet, $F_S = F_T = -8T_D^2 g/(3g_c^S)^2$, see Fig.10b, consistent with the general chemical potential result.

C. The singlet triplet crossover due to exchange interaction.

When the exchange interaction is added perturbatively (at coupling above the critical one for the triplet), the energies of the competing condensates are shifted; the crossover exchange (Stoner) coupling constant I , defined in Eq.(20), is given in Fig. 10 as function of the electron-electron local coupling g . For g just above the critical for triplet g_c^T , see Eq.(50), the value of the I_c is about $I_c = 6$ (in units of $v_F^3 \hbar^3/T_D^2$), so that $I_c = \frac{6}{12\pi^2} = 0.05$. As the phonon mediated attraction strength increases the critical value of exchange decreases as $1/g$. The Dirac superconductor therefore is a rare example of 3D quantum critical point.

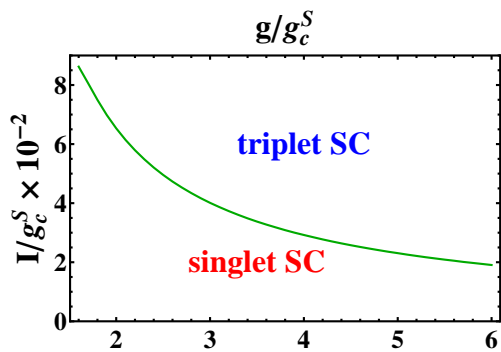


FIG. 11. Critical exchange coupling as function of g at quantum critical point.

VI. DISCUSSION AND CONCLUSIONS.SUMMARY.

To summarize, we have constructed a microscopic theory of superconductivity (at zero temperature) in 3D time reversal and inversion invariant massless Dirac semi - metals. In these materials there are at least two bands of opposite chiralities. Such a band structure appear in many recently studied materials including copper doped TI Bi_2Se_3 in which the triplet superconductivity is suspected¹⁸.

In the framework of the "conventional" phonon mediated local attraction model we classified, under simplifying assumptions of the 3D rotation invariance, inversion and the time reversal, possible pairing channels. There are three singlet channels and one triplet. Comparison of energies of these condensates for arbitrary chemical potential and the electron-electron interaction strength demonstrates that a singlet pairing always prevails, as shown in Fig. 5. However, one notices that in large portions of the phase diagram the energy density differences are much smaller than the typical values of energy densities themselves. This means that interactions that are small but discriminate between the spin singlet and the spin triplet are important in order to determine the nature of the superconducting order there.

The best candidate for such an interaction in materials under consideration is the exchange (the Stoner term). Parameters of the model are therefore the chemical potential μ , the effective electron - electron coupling strength g and the Stoner coupling exchange constant I . Our main results are given in Figs. 8a, 8b and 11. In certain ranges of parameters that include the electron - phonon coupling parametrized by dimensional effective electron - electron coupling λ and the exchange interaction parametrized by λ_{ex} , the triplet pairing is favored over the singlet one. Fig. 8a, 8b demonstrate that the triplet exists either at small chemical potential of order Debye energy T_D or perhaps as small λ and large chemical potential, while the singlet prevails in the upper-right corner of the diagram beyond the red line.

The second region where triplet is competitive happens

to be beyond the range of validity of the perturbation theory and in fact will not materialize since the superconducting order instability is probably weaker than the Stoner instability for ferromagnetic correlations, so we are left with the triplet states when the chemical potential is small.

To this end we have investigated the limit of zero chemical potential, where the tendency towards the triplet pairing should be maximal. This is presented in Fig.11. In this limit one cannot use the dimensionless coupling strengths λ and λ_{ex} , therefore should go back to the dimensional coupling strengths g and I related to the former by Eqs.(27,44) used in this phase diagram. Transition to superconductivity in this case is a rare occurrence of quantum critical point in 3D with distinct critical couplings and exponents.

A. Experimental feasibility of the triplet superconductivity due to phonon and exchange interactions.

To estimate the pairing efficiency due to phonons, one should rely on recent studies²¹. The effective dimensionless electron - electron coupling constant due to phonons λ , defined in Eq.(27), is obtained from the exchange of acoustic phonons and is of order¹⁷ 0.1 - 1 (somewhat lower values are obtained in ref.¹⁶). Note that a reasonable electron density of $n = 3 \cdot 10^{11} cm^{-2}$ in Bi_2Te_3 already conforms to the requirement that chemical potential less than the Debye cutoff energy $T_D = 300K$.

To estimate the strength of the exchange interactions due to itinerant electrons one, as usual, starts from the Coulomb repulsion. The effects of Coulomb interaction in 3D Dirac electrons are being studied extensively⁸. RG analysis reveals the logarithmic divergence of Fermi velocity v_F , while the effective fine structure constant $\alpha = e^2/\hbar v_F$ is marginally irrelevant. When a Dirac point is located on the Fermi level, the Coulomb interaction is not screened. The Stoner theory²² predicts that when λ_{ex} becomes of order 1, the material develops ferromagnetism. Below that only the correlations play a role, but as is seen in Figs.8a-b, such a relatively small exchange is sufficient to damage the singlet condensate in favor of the triplet.

B. Feasibility of observing the quantum criticality.

In this paper we especially focused on the qualitatively distinct case of Dirac fermions with small chemical potential. The situation is quite similar to that of the 2D Weyl semi-metal in topological insulators. Although in the original proposal of TI in materials²⁸ the chemical potential was zero, in experiments one finds often that the Dirac point is shifted away from the Fermi surface by a significant fraction of eV^2 . There are however experimental methods to shift the location of the point

by doping (for example by copper¹³), gating, pressure etc.²⁶. Superconductivity was in fact observed in otherwise non-superconducting TIs Bi_2Te_3 and Bi_2Se_3 under pressure¹⁸ $v_F \approx 7 \cdot 10^5 m/s$ (for Bi_2Se_3). It is possible that at a certain pressure the system passes through the quantum critical point and is therefore a candidate for the maximal enhancement of the triplet superconductivity.

C. Possible generalizations and comparison with other works.

Here we compare our results with the earlier work ref.¹⁹ designed to model the symmetries and parameters of Cu doped Bi_2Se_3 . The case that can be directly compared is when the relativistic mass term (denoted by m in ref.¹⁹) is small compared to chemical potential. In this work a more general effective electron - electron interaction was considered with two couplings V and U for local intraband and interband attractions, respectively. They are related to our g by

$g = 2U = 2V$. Qualitatively, for $U/V = 1$ one gets nearly degenerate energies (critical temperatures were compared in ref.¹⁹ instead). This is similar but not identical to our result without exchange, see Fig. 7. We indeed obtain the degeneracy of the two gaps, the singlet and the triplet (their Δ_1 and Δ_2 respectively), but only in the limit of large g . The gaps are definitely not degenerate when the coupling g is below $20\pi^2 v_F^3 \hbar^2 / T_D^2$. Even within the BCS regime (Eqs.(35,29)), $\Delta_T / \Delta_S = \sinh(0.35/\lambda) / \sinh(0.5/\lambda)$. This is consistent with 1 only for quite large coupling (whatever UV cutoff used in ref.¹⁹).

Acknowledgements. We are indebted to C. W. Luo, J. J. Lin and W.B. Jian for explaining details of experiments, and T. Maniv and M. Lewkowicz for valuable discussions. Work of B.R. and D.L. was supported by NSC of R.O.C. Grants No. 98-2112-M-009-014-MY3 and MOE ATU program. The work of D.L. also is supported by National Natural Science Foundation of China (No. 11274018)

* vortexbar@yahoo.com

† shapib@mail.biu.ac.il

‡ lidp@pku.edu.cn

§ yairaliza@gmail.com

¹ P.A. Wolff, J. Phys. Chem. Sol. **25**, 1057 (1964).

² Z. Hasan and C. L. Kane, Rev. Mod. Phys. **82**, 3045 (2010); X.-L. Qi and S.-C. Zhang, Rev. Mod. Phys. **83**, (2011); B.A. Bernevig, "Topological insulators and topological superconductors", Princeton University Press, Princeton (2013).

³ S. M. Young, S. Chowdhury, E. J. Walter, E. J. Mele, C. L. Kane, and A. M. Rappe, Phys. Rev. B **84**, 085106 (2011).

⁴ Z.Wang, Y. Sun, X.-Q. Chen, C. Franchini, G. Xu, H. Weng, X. Dai, and Z. Fang, Phys. Rev. B **85**, 195320 (2012); P. Hosur, X. Dai, Z. Fang and X.-L. Qi, Time-reversal invariant topological superconductivity in doped Weyl semimetals, arXiv:1405.4299v1.

⁵ Z. K. Liu, B. Zhou, Y. Zhang, Z. J. Wang, H. M. Weng, D. Prabhakaran, S.-K. Mo, Z. X. Shen, Z. Fang, X. Dai, Z. Hussain, Y. L. Chen, Science **343**, 864 (2014); S.-Y. Xu, C. Liu, S. K. Kushwaha, T.-R. Chang, J. W. Krizan, Sankar, C. M. Polley, J. Adell, T. Balasubramanian, K. Miyamoto, N. Alidoust, Guang Bian, M. Neupane, I. Belopolski, H.-T. Jeng, C.-Y. Huang, W.-F. Tsai, H. Lin, F. C. Chou, T. Okuda, A. Bansil, R. J. Cava, and M. Z. Hasan, Observation of a bulk 3D Dirac multiplet, Lifshitz transition, and nested spin states in Na_3Bi . ArXiv 1312.7624 (2013).

⁶ G. Hu, H. Weng, Z. Wang, X. Dai, and Z. Fang, Phys. Rev. Lett. **107**, 186806 (2011); Z. Wang, H. Weng, Q. Wu, X. Dai, and Z. Fang, Phys. Rev. B **88**, 125427 (2013); M. Neupane, et.al. Observation of a topological 3D Dirac semimetal phase in high-mobility Cd_3As_2 , arXiv:1309.7892 (2013).

⁷ M. Orlita, D. M. Basko, M. S. Zholudev, F. Teppe, W. Knap, V. I. Gavrilenco, N. N. Mikhailov, S. A. Dvoretzkii,

P. Neugebauer, C. Faugeras, A-L. Barra, G. Martinez and M. Potemski, Nat. Phys. **10**, 233 (2014).

⁸ Y. Fuseya, M. Ogata, and H. Fukuyama, Phys. Rev. Lett. **102**, 066601 (2009); P. Hosur, S. A. Parameswaran, and A. Vishwanath, Phys. Rev. Lett. **108**, 046602 (2012); M. Lewkowicz and B. Rosenstein, Phys. Rev. B **88**, 045108 (2013).

⁹ S. M. Young, S. Zaheer, J. C.Y. Teo, C. L. Kane, E. J. Mele, and A. M. Rappe, Phys. Rev. Lett. **108**, 140405 (2012).

¹⁰ P. Hosur, S. Ryu, A. Vishwanath, Phys. Rev. B **81**, 045120 (2010); X. Wan, A. M. Turner, A. Vishwanath, and S. Y. Savrasov, Phys. Rev. B **83**, 205101 (2011); W. Witczak-Krempa and Y. B. Kim, Phys. Rev. B **85**, 045124 (2012).

¹¹ T. Kariyado and M. Ogata: J. Phys. Soc. Jpn. **80**, (2011); **81**, 064701 (2012); P. Delplacel, J. Li and D. Carpentier, Europhys. Lett. **97**, 67004 (2012).

¹² T. Timusk and J. P. Carbotte, C. C. Homes, D. N. Basov and S. G. Sharapov, Phys. Rev. B **87**, 235121 (2013).

¹³ Y. S. Hor, A. J. Williams, J. G. Checkelsky, P. Roushan, J. Seo, Q. Xu, H. W. Zandbergen, A. Yazdani, N. P. Ong, and R. J. Cava, Phys. Rev. Lett. **104**, 057001 (2010).

¹⁴ X. Zhu, L. Santos, R. Sankar, S. Chikara, C. Howard, F.C. Chou, C. Chamon, M. El-Batanouny, Phys. Rev. Lett. **107**, 186102 (2011); C. W. Luo, H. J. Wang, S. A. Ku, H.-J. Chen, T. T. Yeh, J.-Y. Lin, K. H. Wu, J. Y. Juang, B. L. Young, T. Kobayashi, C.-M. Cheng, C.-H. Chen, K.-D. Tsuei, R. Sankar, F. C. Chou, K. A. Kokh, O. E. Tereshchenko, E. V. Chulkov, Yu. M. Andreev, and G. D. Gu, Nano Lett. **13**, 5797 (2013); X. Zhu, L. Santos, C. Howard, R. Sankar, F.C. Chou, C. Chamon, M. El-Batanouny, Phys. Rev. Lett. **108**, 185501 (2012).

¹⁵ S. Das Sarma and Q. Li, Phys. Rev. B **88**, 081404(R) (2013).

¹⁶ Z.-H. Pan, A. V. Fedorov, D. Gardner, Y. S. Lee, S. Chu,

- T. Valla, Phys. Rev. Lett. **108**, 187001 (2012); V. Parente, A. Tagliacozzo, F. von Oppen, and F. Guinea, Phys. Rev. B **88**, 075432 (2013).
- ¹⁷ M. N. Ali, Quinn D. Gibson, T. Klimczuk, and R. J. Cava, Phys. Rev. B **89**, 020505(R) (2014).
- ¹⁸ J. J. Hamlin, J. R. Jeffries, N. P. Butch, P. Syers, D. A. Zocco, S. T. Weir, Y. K. Vohra, J. Paglione, and M. B. Maple, J. Phys. Cond. Mat. **24**, 035602 (2012); K. Kirshenbaum, P. S. Syers, A. P. Hope, N. P. Butch, J. R. Jeffries, S. T. Weir, J. J. Hamlin, M. B. Maple, Y.K. Vohra, and J. Paglione, Phys. Rev. Lett. **111**, 087001 (2013).
- ¹⁹ L. Fu and E. Berg, Phys. Rev. Lett. **105**, 097001 (2010)
- ²⁰ C.-K. Lu and I. F. Herbut, Phys. Rev. B **82**, 144505 (2010); B. Roy, V. Juricic, and I. F. Herbut, Phys. Rev. B **87**, 041401 (2013).
- ²¹ P. M. R. Brydon, S. Das Sarma, H.-Y. Hui, and J. D. Sau, Odd-parity superconductivity from phonon-mediated pairing, arXiv:1402.7061v1 (2014).
- ²² R. M. White, "Quantum theory of magnetism", Springer-Verlag, Heidelberg (1983).
- ²³ S. Sachdev, "Quantum Phase Transitions", Second Edition, Cambridge University Press (2011).
- ²⁴ P. A. Lee, N. Nagaosa, X.-G. Wen, Rev. Mod. Phys. **78**, 17 (2006).
- ²⁵ D. Li, B. Rosenstein, I. Shapiro, B. Ya. Shapiro, "Quantum critical point in the superconducting transition on the surface of topological insulator", arXiv:submit/0985109 (2014).
- ²⁶ J. G. Checkelsky, Y. S. Hor, R. J. Cava, and N. P. Ong, Phys. Rev. Lett. **106**, 196801 (2011); D. Kim, S. Cho, N. P. Butch, P. Syers, K. Kirshenbaum, S. Adam, J. Paglione and M. S. Fuhrer, Nat. Phys. **8**, 459 (2012).
- ²⁷ A. A. Abrikosov, L. P. Gor'kov, I. E. Dzyaloshinskii, "Quantum field theoretical methods in statistical physics", Pergamon Press, New York (1965).
- ²⁸ H. Zhang, C.-X. Liu, X.-L. Qi, X. Dai, Z. Fang, and S.-C. Zhang, Nat. Phys. **5**, 438 (2009).